Appendix A.

Table 7 introduces the basic notations and decision variables in our mathematical formulation.

Table 7: Sets, parameters, and decision variables for the proposed formulation

Notations	Definitions
Symbols and parameters	
L	Set of lines in the rail transit network, indexed by l and l'
S_l	Set of stations on line l
S	Set of involved stations in the rail transit network
$T = \{0, 1, \cdots\}$	Set of discrete time units in the considered time horizon
$\mathcal{P}$	Set of feasible travelling paths of passengers
t_i^d	Dwell time of each train at station i
t_i^r	Running time of each train between stations i and $i+1$
t_{ij}^s	Passenger transfer time between connected stations i and j
D_p^t	Number of passengers with path p entering the network at time t
SC_i	Loading capacity of station i
C	Loading capacity of each train
T_{min}^l	Minimum headway time of line l
T_{cycle}^l	Cycle time of line l (the time that each train requires to return to the origin station)
K_l	Fleet size of line l
Decision variables	
x_{lt}	Binary decision variable, =1 if a train departs from the depot of line l at time t; =0 otherwise.
n_i^t	Number of waiting passengers at station i and time t
b_{pi}^t	Number of boarding passengers with travel path p at station i and time t

Appendix B.

This appendix gives the proof of Lemma 3.1.

Proof. First, as the original CTT model has a *max-min* objective function, it can be equivalently reformulated as follows by introducing a continuous variable ξ, i.e.,

$$\min_{x,\xi} \quad \xi \tag{31}$$

$$\text{s.t.} \quad \xi \geq \frac{n_i}{SC_i}, \quad \forall i \in S, t \in T \tag{32}$$

$$\text{Constraints } (8) - (16), (18)$$

$$\xi \geq 0. \tag{33}$$

Next, we show that variables n_i^t, constraints (8) and constraints (16) can be further eliminated. We note that constraints (8)

$$n_i^t = \sum_{\tau \in T_t} d_i^\tau + \sum_{p \in \mathcal{P}_i^r} \sum_{\tau \in T_{pit}} b_{pi_p^+}^\tau - \sum_{\tau \in T_t} \sum_{p \in \mathcal{P}_i^o \cup \mathcal{P}_i^r} b_{pi}^\tau, \qquad \forall i \in S, t \in T$$

and constraints (16) (i.e., $n_i^t \geq 0$ for $\forall i, t$) are equivalent to stating that the right term of (8) is non-negative. Therefore, if we could prove that the right term of (8) is no less than zero, then we can prove that variables n_i^t and constraints (8) and constraints (16) are redundant, thus proving Lemma reformulation.

According to (10) and (11), we have

$$\sum_{\tau\in T_t} d_i^\tau + \sum_{p\in\mathcal{P}_i^r}\sum_{\tau\in T_{pit}} b^\tau_{pi^+_p} - \sum_{\tau\in T_t}\sum_{p\in\mathcal{P}_i^o\cup\mathcal{P}_i^r} b^\tau_{pi} \tag{34}$$

$$\geq \sum_{\tau\in T_t} d_i^\tau + \sum_{p\in\mathcal{P}_i^r}\sum_{\tau\in T_{pit}} b^\tau_{pi^+_p} - \Big(\sum_{p\in\mathcal{P}_i^o}\sum_{\tau\in T_t} D_p^\tau + \sum_{p\in\mathcal{P}_i^r}\sum_{\tau\in T_{pit}} b^\tau_{pi^+_p}\Big) \tag{35}$$

$$= \sum_{\tau\in T_t} d_i^\tau - \sum_{p\in\mathcal{P}_i^o}\sum_{\tau\in T_t} D_p^\tau \geq 0. \tag{36}$$

The above inequalities demonstrate that constraints (10) and (11) guarantee $\sum_{\tau\in T_t} d_i^\tau + \sum_{p\in\mathcal{P}_i^r}\sum_{\tau\in T_{pit}} b^\tau_{pi^+_p} - \sum_{\tau\in T_t}\sum_{p\in\mathcal{P}_i^o\cup\mathcal{P}_i^r} b^\tau_{pi} \geq 0$, which completes the proof. □

Appendix C.

Equation (37)-(44) is a linear programming model, which uses $\bar{x}_{lt}, \forall i \in L, t \in T$ as input (i.e., the train timetable is fixed in this optimization problem) and minimizes the total waiting time of passengers. Note that (37) actually minimizes the total waiting time of passengers under the assumption that the time horizon is discretized into equivalent time units, as indicated, e.g., in Barrena et al. (2014a) and Yin et al. (2017). The other decision variables and the parameters are the same as those presented in our CTT formulation, and thus we refer the reader to Section 3 for more information.

$$\min_{b,n} \quad \sum_{i\in S}\sum_{t\in\mathcal{T}} n_i^t, \tag{37}$$

$$\text{s.t. } n_i^t = \sum_{\tau\in T_t} d_i^\tau + \sum_{p\in\mathcal{P}_i^r}\sum_{\tau\in T_{pit}} b^\tau_{pi^+_p} - \sum_{\tau\in T_t}\sum_{p\in\mathcal{P}_i^o\cup\mathcal{P}_i^r} b^\tau_{pi}, \qquad \forall i\in S, t\in T \tag{38}$$

$$\sum_{p\in\mathcal{P}_i} b^t_{pi} \leq C\cdot \bar{x}_{l(t-t_i)}, \qquad \forall i\in S_l, l\in L, t\in T: t\geq t_i \tag{39}$$

$$\sum_{p\in\mathcal{P}_i} b^t_{pi} \leq C - \sum_{i'\in S_{il}}\sum_{p'\in\mathcal{P}_{i'i}} b^{t(i',i)}_{pi'}, \qquad \forall i\in S_l, l\in L, t\in T_{pi} \tag{40}$$

$$\sum_{\tau\in T_t} b^\tau_{pi} \leq \sum_{\tau\in T_t} D_p^\tau, \qquad \forall i\in S_l, p\in\mathcal{P}_i^o, t\in T_{pi} \tag{41}$$

$$\sum_{\tau\in T_t} b^\tau_{pi} \leq \sum_{\tau\in T_{pit}} b^\tau_{pi^+_p}, \qquad \forall i\in S_p^r, p\in\mathcal{P}_i^r, t\in T_{pi} \tag{42}$$

$$b^t_{pi} \geq 0, \qquad \forall p\in\mathcal{P}, i\in S, t\in T \tag{43}$$

$$n_i^t \geq 0, \qquad \forall i\in S, t\in T \tag{44}$$

Appendix D.

Algorithm 2 presents the implementation procedure of DALNS.

Appendix E.

Figure 13 presents the generated TAH, NCT and coordinated train timetable solutions for the two considered lines. Figure 14 presents the variation of crowdedness for each station by adopting the three computed timetables[2]. From these figures, we can see clearly that timetable coordination can remarkably reduce the passenger volume at stations with large passenger flows.

[2]It is worth to note that the plots (a)-(d) of Figure 14 are appeared in (Yin et al., 2019) and are repeated here for the performance comparison between different approaches.

Algorithm 2 Implementation procedure of DALNS

Step 1. (Initialization) Input the basic parameters, including the metro network parameters, maximum numbers of fleet size of each line, minimum headway time, planning time horizon and parameters associated with DALNS.

Step 2. (Initial solution) Use the default MIP solver to solve model (24) - (27) for each $l \in L$ and thus to generate the initial solution x_0. Set the current solution x_c and best solution x_B as:

$$x_c \leftarrow x_0 \text{ and } x_B \leftarrow x_0.$$

Step 3. (ALNS) While the stopping criterion is not met, do:

Step 3.1 Randomly choose a destroy operator to move from the current solution to a new solution $DES(x_c)$ in its neighborhood;

Step 3.2 Randomly choose a repair operator to move from the current solution to a new solution $REP(DES(x_c))$ in its neighborhood;

Step 3.3 Use Algorithm 1 to test the feasibility of $REP(DES(\bar{x}))$.

(a) If the solution is feasible, set the new current solution $\bar{x}' \leftarrow REP(DES(\bar{x}))$;

(b) Otherwise, use Algorithm 1 to generate a new solution $\bar{x}' \leftarrow REP(DES(\bar{x}))$.

Step 3.4 Use the LP solver to solve problem $P(\bar{x}')$ to obtain the objectivve value (i.e., the value of ξ under $\bar{x}'$).

(a) Update the scores and weights according to Eqs. (28)-(29);

(b) If the value of ξ is reduced, compare it to that of the best known solution x_B; set $x_B \leftarrow \bar{x}'$, update the scores and weights according to Eqs. (28)-(29) and go back to Step 3;

(c) Otherwise, check the alternating criteria. If both of them are met, break and go to Step 4; continue otherwise.

Step 4. (DALNS) Input the candidate (feasible) solution $\bar{x}'$ and randomly choose $\bar{l} \in L$;

Step 4.1 Solve $P(\bar{x}', \bar{l})$ to optimality with the MIP solver to obtain the optimal value $J(\bar{x}', \bar{l})$;

(a) If the solution is improved (i.e., a better solution $\hat{x}$ is found), return $\hat{x}$ as a candidate solution to Step 3

(b) Otherwise, go to Step 4.2

Step 4.2 Set $L \leftarrow L \backslash \bar{l}$;

(a) If $L = \emptyset$, go to Step 5 to output the best found solution.

(b) Otherwise, go back to Step 4.

Step 5. Output $\bar{x}'$ as the best found solution to problem (P).

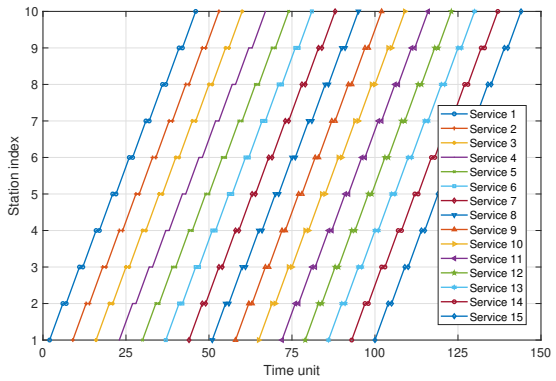

(a) TAH of Line A

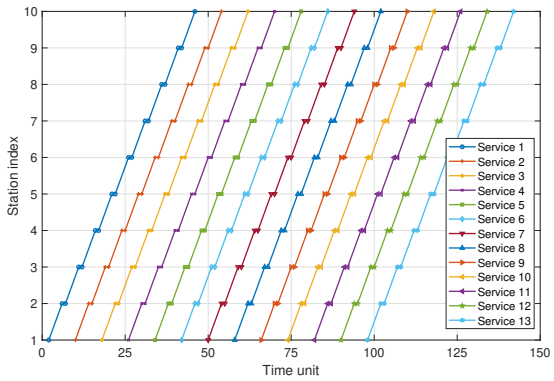

(b) TAH of Line B

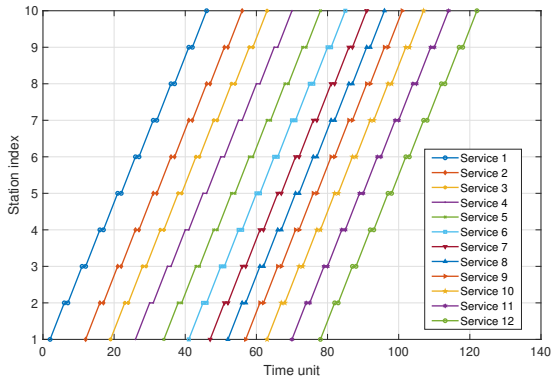

(c) NCT of Line A

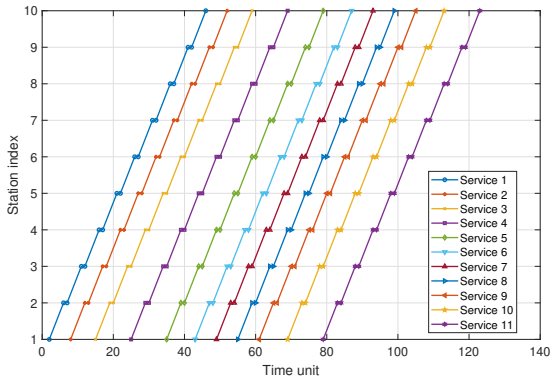

(d) NCT of Line B

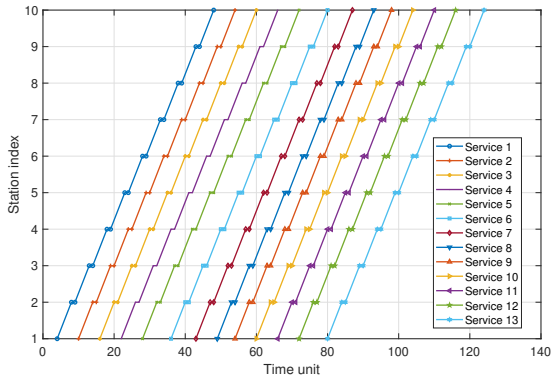

(e) Coordinated timetable of Line A

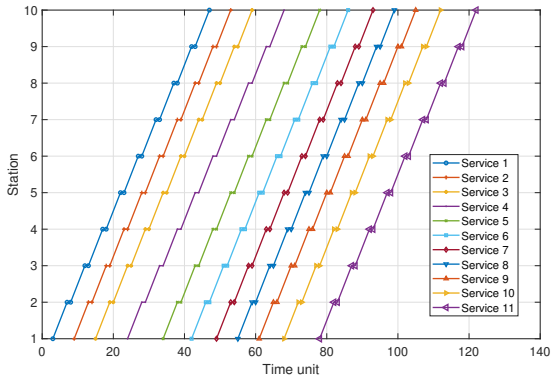

(f) Coordinated timetable of Line B

Figure 13: TAH, NCT versus coordinate timetables for Line A and Line B ((Yin et al., 2019))

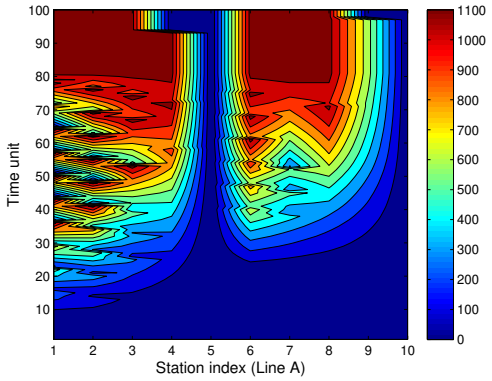

(a) Passenger volume of Line A with TAH

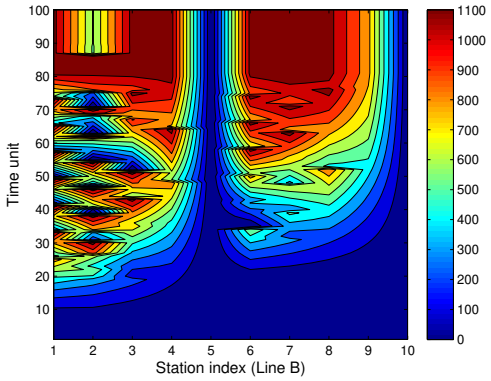

(b) Passenger volume of Line B with TAH

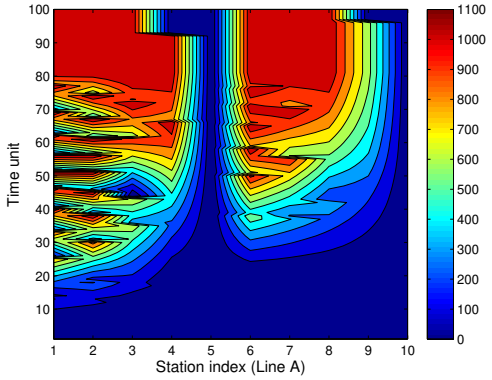

(c) Passenger volume of Line A with NCT

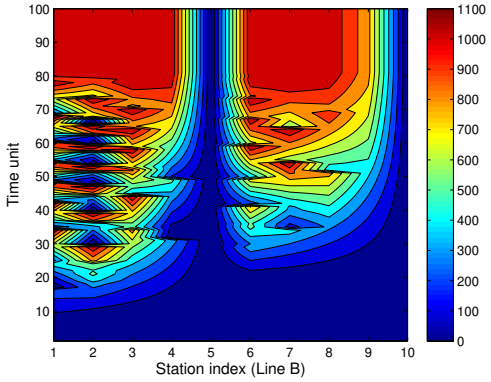

(d) Passenger volume of Line B with NCT

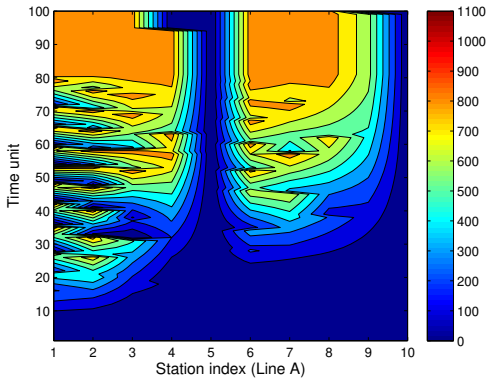

(e) Passenger volume of Line A with coordinated timetable

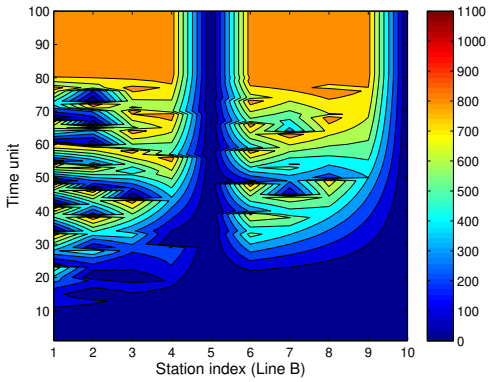

(f) Passenger volume of Line B with coordinated timetable

Figure 14: Passenger volume variations at stations with TAH, NCT and coordinated timetable

Table 8: Departure time of the train services by TAH, NCT and coordinated timetable

	Line A			Line B		
Service index	TAH	NCT	Coordinated timetable	TAH	NCT	Coordinated timetable
1	0	1	2	0	3	1
2	7	6	8	8	9	7
3	14	12	14	16	15	13
4	21	24	20	24	23	22
5	28	32	26	32	33	32
6	35	39	34	40	41	40
7	42	45	41	48	47	47
8	49	50	47	56	53	53
9	56	55	52	64	59	59
10	63	61	58	72	67	66
11	70	68	64	80	77	76
12	77	76	70	88		
13	84	87	78	96		
14	91	92				
15	98					

Appendix F.

Table 8 presents the detailed train service departure time (unit: each 30 seconds) by TAH, NCT and the coordinated train timetable for Line A and Line B.

Appendix G.

Table 9 gives the operational parameters (involving the train running time on each segment, the train dwell time at each station, the planned transfer time at each transfer station) associated with Line No. 8, Line No. 13 and Line Changping in Beijing metro.

Table 9: Operational parameters of Line No. 8, Line No. 13, and Line Changping in Beijing metro

Line No. 8									
Station index	ZXZ	YZL	PXF	HLGD	YX	XXK	YTZ	LCQ	SGFP
Dwell time	50	30	30	30	30	30	30	30	30
Running time	150	150	150	150	150	90	150	210	210
Station index	OG	OSC	BTC	AHQ	ADLB	GLDJ	SCH	NLGX	CAM
Dwell time	30	30	30	30	30	30	30	30	30
Running time	90	150	90	90	90	150	100	150s	180
Station index	ZXC (Line 8 to Line Changping)						HY (Line 8 to Line 13)		
Transfer time	350						300		

Line No. 13								
Station index	XZM	DZS	ZCL	WDK	SD	XEQ	LZ	HLG
Dwell time	50	30	30	30	30	30	30	30
Running time	150	90	150	320	150	250	90	150
Station index	HY	LSQ	BY	WJW	SYJ	GXM	LF	DZM
Dwell time	30	30	50	30	30	30	30	30
Running time	250	150	380	150	90	90	90	180
Station index	XEQ (Line 13 to Line Changping)						HY (Line 13 to Line 8)	
Transfer time	350						300	

Line Changping												
Station index	CPX	MT	CP	CPD	BSW	NS	SHUP	SH	ZHC	ZXZ	ZXZ	XEQ
Dwell time	50	30	30	30	30	30	30	30	30	30	30	30
Running time	210	120	180	320	310	280	140	130	240	170	310	220
Station index	ZXZ (Line Changping to Line 8)							XEQ (Line Changping to Line 13)				
Transfer time	350							300				

Appendix H.

Figures 15 - 18 present the evolution process regarding the number of waiting passengers for two timetables of Table 5 (i.e., for instances D6 and L3). Figures 15 and 16 report the number of waiting passengers at four stations (i.e., stations 1, 2, 3, and 4) of Changping Line and Line 8 for instance L3. As shown in Figure 15, the most congested situations in Changping Line occur at stations 1 and 3 during 7:30 am and 8:00 am. In these situations, a significant number of passengers cannot board the first coming train and those stations become oversaturated quickly. Specifically, the number of waiting passengers at station 1 is even up to 2000 when the practical timetable is applied. However, when the optimized timetables (obtained by ALNS and DALNS) are considered, the crowdedness at station 1 is significantly reduced, which is consistent with the proposed methodology. When the time period approaches 9:00 am, the number of waiting passengers reduces sharply, due to much less passengers entering station 1. It is worth to note that there are very few waiting passengers at the studied stations at the end of the time period for all the timetables (compared with the total number of passengers reported in Table 4). Those waiting passengers will be served by the train services scheduled in the next time period. Moreover, the number of waiting passengers at other less crowed stations (e.g., station 4 in Figure 15 and stations 1-4 in Figure 16) shows that the optimized timetables (by ALNS and DALNS) do not generate a significantly large unsatisfied passenger demand. Similar observations can be drawn for the results obtained for instance D6 in Figures 17 and 18.

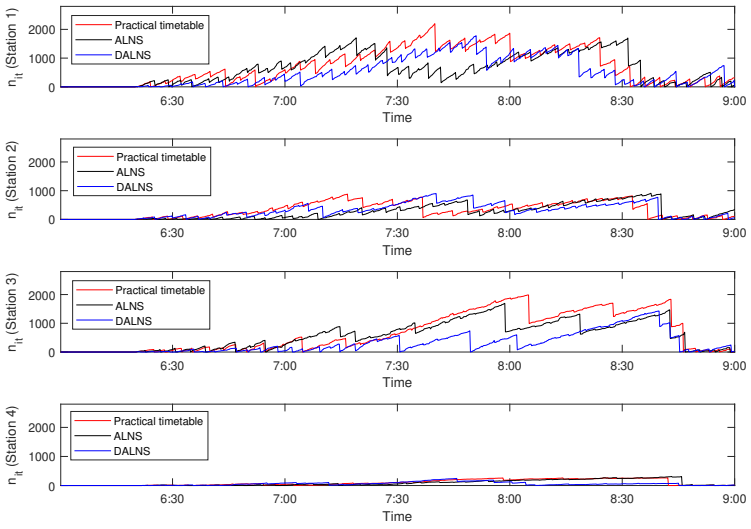

Figure 15: Number of waiting passengers at four stations in Changping Line for instance L3

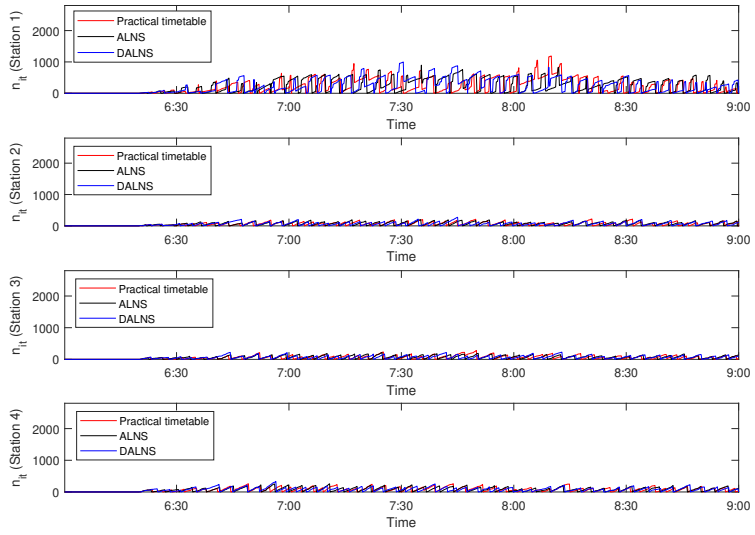

Figure 16: Number of waiting passengers at four stations in Line 8 for instance L3

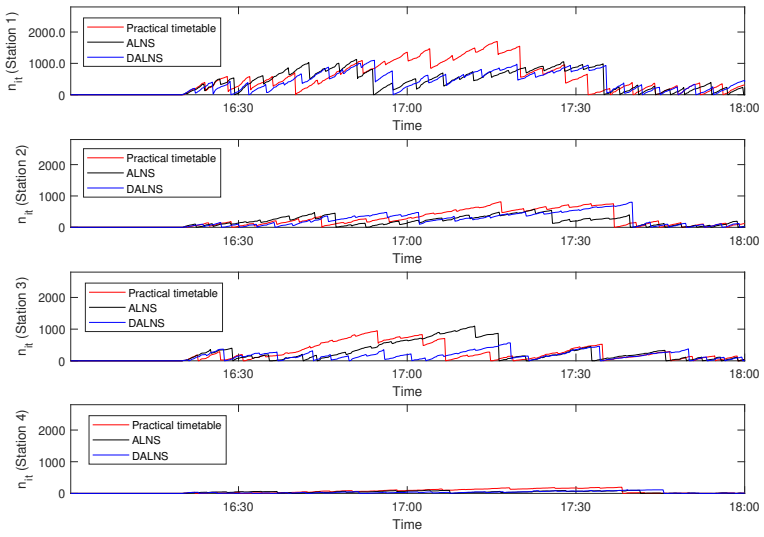

Figure 17: Number of waiting passengers at four stations in Changping Line for instance D6

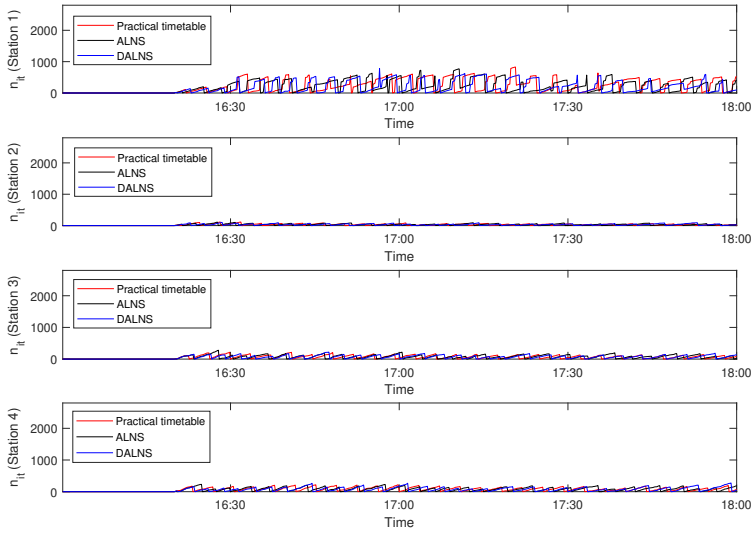

Figure 18: Number of waiting passengers at four stations in Line 8 for instance D6